PHYSICAL LUMPING METHODS FOR DEVELOPING LINEAR REDUCED MODELS FOR HIGH SPEED PROPULSION SYSTEMS

S. M. Immel, T. T. Hartley, J. A. De Abreu Garcia
Department of Electrical Engineering
The University of Akron
Akron, OH 44325-3904
(216) 972-7649
December 1991

ABSTRACT

In gasdynamic systems, information travels in one direction for supersonic flow and in both directions for subsonic flow. A shock occurs at the transition from supersonic to subsonic flow. Thus, to simulate these systems, any simulation method implemented for the quasi-one-dimensional Euler equations must have the ability to capture the shock. In this paper, a technique combining both backward and central differencing is presented. The equations are subsequently linearized about an operating point and formulated into a linear state space model. After proper implementation of the boundary conditions, the model order is reduced from 123 to less than 10 using the Schur method of balancing. Simulation results comparing frequency and step responses of the reduced order models and the original system model are presented. This paper essentially follows the approach of Chicatelli, 1990, and Chicatelli and Hartley, 1990, while using an alternative for the flux splitting method.

INTRODUCTION

The digital simulation of gasdynamic systems is typically complex and computer intensive. Furthermore, gasdynamic systems have general characteristics which must be accounted for when choosing a simulation method. One major characteristic to be considered is that in gasdynamic systems, there are regions of supersonic flow and subsonic flow. In a one-dimensional problem, regions of supersonic flow will exhibit travelling of information in one direction. On the other hand, regions of subsonic flow will have information travelling in two opposing directions. The discontinuity occurring at this transition from supersonic flow to subsonic flow is called a shock. A shock generally appears in any physical system where there is a substantial transfer of energy from one form to another. In these systems, shock position is usually the desired control variable because of its physical significance. Consequently, any simulation method used must have the ability to accurately track the shock position. This specific consideration will be discussed later in the paper, but first consider a general discussion on the simulation of gasdynamic systems.

A popular simulation approach for partial differential equations is the finite differencing technique. However, spatial differencing on distributed partial differential equations requires some general knowledge of system behavior. Moreover, the effects of the differencing method on the simulation must be considered. Since forward or backward differencing allows information to flow in only one direction, either method leads to numerical instabilities for systems containing subsonic flow. Thus, forward and backward differencing are, by themselves, not suitable simulation techniques for gasdynamic systems. On the other hand, although central differencing permits the flow of information in both directions it typically leads to unstable difference equations and/or simulations corrupted with high frequency spurious noise [3]. The foregoing suggests that, to simulate gasdynamic systems, one may consider a method which combines forward or backward differencing with central differencing. However, it should be born in mind that, assumptions about information flow direction must be made.

The simulation method implemented in this paper is essentially a modification of a method developed by Courant, Isaacson, and Rees [4] and Roache [7]. This method considers the actual physics of the gasdynamic process when performing the spatial differencing. Mass flow and energy are assumed to propagate signals downstream. Therefore, only backward differencing is used in these two equations. Any term associated with system pressure is assumed to communicate information in both directions. Thus, pressure terms are estimated using central differencing. It turns out that this method has the ability to capture the shock, remain stable, and provide accurate results [3]. Since it performs the differencing based on fundamental physics, the method is referred to as physical lumping. This technique is applied to the general quasi-one-dimensional gasdynamic equations for density, mass flow, and energy. Once this spatial differencing scheme is applied, the gasdynamic equations are subsequently linearized about a steady state operating point.

The specific system under consideration is the NASA Lewis 40-60 Inlet [8]. This physical system may be represented by 41 spatial lumps approximately 0.1427 feet apart. Considering that there are three governing equations for each spatial lump, the overall system is 123rd order. Since the dynamics at each lump are only a function of the previous lump and the next lump, the structure of the model lends itself to a tridiagonal state space formulation. This high order state space representation is then reduced using the Schur method of balancing [5].

The Schur method of balancing and its use in model reduction were first presented in [5]. In this truncation based model reduction method, the first concern is the size of the characteristic Hankel singular values (HSV). Typically, any large break in the HSVs, usually taken as a 10 to 1 ratio, is a feasible position to truncate the model in balanced coordinates. The resulting reduced order model (ROM) must then be studied to ensure

that all desired characteristics of the linear full order model (LFOM) and the nonlinear full order model (NLFOM) are retained. In this paper, 4th and 6th order linear ROMs are calculated. The step responses and frequency responses of these ROMs are considered.

NASA Lewis 40-60 Inlet

The starting point for the analysis begins with the three governing nonlinear quasi-one-dimensional gasdynamic equations for continuity, conservation of momentum, and conservation of energy. These equations, referred to as the Euler equations, are

Continuity:

$$\frac{\partial(\rho A)}{\partial t} + \frac{\partial(\rho u A)}{\partial x} = M_s \tag{1}$$

Conservation of Momentum:

$$\frac{\partial(\rho u A)}{\partial t} + \frac{\partial[A(P+\rho u^2)]}{\partial x} = P\frac{\partial A}{\partial x} + F_s \tag{2}$$

and Conservation of Energy:

$$\frac{\partial(EA)}{\partial t} + \frac{\partial[Au(E+P)]}{\partial x} = -P\frac{\partial A}{\partial t} + Q_s \tag{3}$$

with

$$P = 0.4\left(E - \frac{m^2}{2\rho}\right). \tag{4}$$

The major variables of concern are

$\rho \equiv$ density
$u \equiv$ velocity
$P \equiv$ pressure
$E \equiv$ energy
$A \equiv$ area.

The velocity may be expressed in terms of the mass flow and the density as

$$u = \frac{m}{\rho}. \tag{5}$$

Furthermore, the general gasdynamic equations may be written in terms of ρ, m, E, and P. The terms M_s, F_s, and Q_s are the input source terms. For the specific problem considered here, inputs will be applied at the boundary conditions. After this simplification, the system equations may then be expressed by finite difference terms.

The spatial differencing method implemented in this paper applies backward differencing on the mass flow and energy terms since they are considered to flow in only one direction. On the other hand, central differencing is applied to any pressure-related terms since they are considered to propagate in both directions. Thus, the equations for density, mass flow, and energy are first discretized in space as

$$\dot{\rho}_i = -\frac{1}{HA_i}[A_i m_i - A_{i-1} m_{i-1}] + \left(\frac{1}{A_i}\right) M_i$$

$$\dot{m}_i = -\frac{1}{HA_i}\left[\frac{A_i m_i^2}{\rho_i} - \frac{A_{i-1} m_{i-1}^2}{\rho_{i-1}}\right] - \frac{1}{2HA_i}[P_{i+1}A_{i+1} - P_{i-1}A_{i-1}] + \frac{P_i}{A_i}\left[\frac{dA}{dx}\right]_i + \left(\frac{1}{A_i}\right) F_i$$

$$\dot{E}_i = -\frac{1}{HA_i}\left[\frac{A_i m_i E_i}{\rho_i} - \frac{A_{i-1} m_{i-1} E_{i-1}}{\rho_{i-1}}\right] - \frac{1}{2HA_i}\left[\frac{A_{i+1} m_{i+1} P_{i+1}}{\rho_{i+1}} - \frac{A_{i-1} m_{i-1} P_{i-1}}{\rho_{i-1}}\right] + \left(\frac{1}{A_i}\right) Q_i . \tag{6}$$

The NASA Lewis 40-60 inlet may be represented by 41 spatial lumps with a spatial step, H = 0.1427 feet as in [1]. This in turn results in a 123rd order model. It should be noted that this specific method uses Euler's method to approximate the time derivatives. To expedite the analysis process, and to keep from adding a dynamic equation for pressure, the system equations must be further simplified.

All of the pressure variables shown in (6) may be expressed in terms of the relationship shown in (4). Subsequently, (6) may then be rewritten as follows

$$\dot{\rho}_i = \frac{A_{i-1} m_{i-1}}{HA_i} - \frac{m_i}{H}$$

$$\dot{m}_i = -\frac{m_i^2}{H\rho_i} + \frac{A_{i-1} m_{i-1}^2}{HA_i \rho_{i-1}} + \frac{0.2 A_{i-1} E_{i-1}}{HA_i} - \frac{0.1 A_{i-1} m_{i-1}^2}{HA_i \rho_{i-1}} - \frac{0.2 A_{i+1} E_{i+1}}{HA_i} + \frac{0.1 A_{i+1} m_{i+1}^2}{HA_i \rho_{i+1}} + \left(\frac{0.4 E_i}{A_i} - \frac{0.2 m_i^2}{\rho_i A_i}\right)\left[\frac{dA}{dx}\right]_i$$

$$\dot{E}_i = \frac{1.2 A_{i-1} m_{i-1} E_{i-1}}{HA_i \rho_{i-1}} - \frac{m_i E_i}{H\rho_i} - \frac{0.1 A_{i-1} m_{i-1}^3}{HA_i \rho_{i-1}^2} - \frac{0.2 A_{i+1} m_{i+1} E_{i+1}}{HA_i \rho_{i+1}} + \frac{0.1 A_{i+1} m_{i+1}^3}{HA_i \rho_{i+1}^2} . \tag{7}$$

Equation (7) can now be implemented as a shock capturing computational fluid dynamics (CFD) scheme for the quasi-one-dimensional Euler equations. The resulting model can be used for control evaluation in a real-time simulation and thus for control system design.

The next step is to linearize equation (7) about a steady state operating point in order to develop a model for controller design. However, it is necessary to first consider the structural properties of (7). Recall that the 40-60 inlet is comprised of 41

spatial lumps with three governing equations for each lump, namely, density, mass flow, and energy. The structure of these equations enables the construction of a large linear state space model. Suppose a state vector is defined as

$$x^T = [\rho_1\ m_1\ E_1 \vdots \rho_2\ m_2\ E_2 \vdots \ldots \vdots \rho_{41}\ m_{41}\ E_{41}]. \tag{8}$$

Following this definition of x, the system may be put into the general state space form

$$\begin{aligned} \dot{x} &= Ax + Bu \\ y &= Cx. \end{aligned} \tag{9}$$

Since the dynamics of the system are a function of the present state and the states to the left and right, the A matrix has a tridiagonal form and may be constructed as

$$A = \begin{bmatrix} J_1 & Q_2 & 0 & 0 & . & . & . & 0 \\ P_1 & J_2 & Q_3 & 0 & . & . & . & 0 \\ 0 & P_2 & J_3 & Q_4 & . & . & . & 0 \\ . & & & . & & & & . \\ . & & & & . & & & . \\ . & & & & & . & & . \\ 0 & 0 & . & . & . & P_{n-2} & J_{n-1} & Q_n \\ 0 & 0 & 0 & . & . & . & P_{n-1} & J_n \end{bmatrix}. \tag{10}$$

Notice that the first and last rows do not include a P_i and Q_j term respectively. The effect of these matrices must be considered when applying any boundary conditions to the system as will be seen later in the paper. Taken directly as the small perturbation linearization of the discrete space equations given in (7), the P_i, J_i, and Q_i matrices shown in (10) are

$$J_i = \left[\begin{array}{c|c|c} 0 & -\frac{1}{H} & 0 \\ \hline \frac{m_i^2}{H\rho_i^2} + \frac{0.2m_i^2}{\rho_i^2 A_i}\left[\frac{dA}{dx}\right]_i & \frac{-2m_i}{H\rho_i} - \frac{0.4m_i}{\rho_i A_i}\left[\frac{dA}{dx}\right]_i & \frac{0.4}{A_i}\left[\frac{dA}{dx}\right]_i \\ \hline \frac{m_i E_i}{H\rho_i^2} & -\frac{E_i}{H\rho_i} & -\frac{m_i}{H\rho_i} \end{array}\right] \tag{11}$$

$$P_i = \begin{bmatrix} 0 & \frac{A_i}{HA_{i+1}} & 0 \\ -\frac{A_i m_i^2}{HA_{i+1}\rho_i^2} + \frac{0.1A_i m_i^2}{HA_{i+1}\rho_i^2} & \frac{1.8A_i m_i}{HA_{i+1}\rho_i} & \frac{0.2A_i}{HA_{i+1}} \\ \frac{0.2A_i m_i^3}{HA_{i+1}\rho_i^3} - \frac{1.2A_i m_i E_i}{HA_{i+1}\rho_i^2} & \frac{1.2A_i E_i}{HA_{i+1}\rho_i} - \frac{0.3A_i m_i^2}{HA_{i+1}\rho_i^2} & \frac{1.2A_i m_i}{HA_{i+1}\rho_i} \end{bmatrix} \tag{12}$$

$$Q_i = \begin{bmatrix} 0 & 0 & 0 \\ -\frac{0.1A_i m_i^2}{HA_{i-1}\rho_i^2} & \frac{0.2A_i m_i}{HA_{i-1}\rho_i} & -\frac{0.2A_i}{HA_{i-1}} \\ -\frac{0.2A_i m_i^3}{HA_{i-1}\rho_i^3} + \frac{0.2A_i m_i E_i}{HA_{i-1}\rho_i^2} & -\frac{0.2A_i E_i}{HA_{i-1}\rho_i} + \frac{0.3A_i m_i^2}{HA_{i-1}\rho_i^2} & -\frac{0.2A_i m_i}{HA_{i-1}\rho_i} \end{bmatrix}. \tag{13}$$

The measured output is the change in pressure, δP, directly downstream of the shock. The position of the shock is directly related to the change in pressure at this position [6]. As the steady state shock position in the 40-60 inlet is located around the 24th lump, the C matrix for the output δP may be constructed as

$$C = \left[0 \; 0 \; . \; . \; . \; 0 \; \frac{0.2m_{24}^2}{\rho_{24}^2} \; \frac{-0.4m_{24}}{\rho_{24}} \; 0.4 \; 0 \; . \; . \; . \; 0 \right]. \tag{14}$$

The input to the system will be a change in pressure at the farthest point downstream corresponding to the last physical lump. This input is introduced into the system model by the B matrix. However, the effects of the boundary conditions should be considered first. Boundary conditions for this problem must take care of introducing a reflection in pressure information at the last lump. Consequently, the last row of the A matrix must be changed. The last row of the small perturbation model, with corresponding subscripts for elements in P and Q, is given as

$$\begin{aligned} \delta\dot{E}_{41} = {} & (P_{40})_{3,1}\delta\rho_{40} + (P_{40})_{3,2}\delta m_{40} + (P_{40})_{3,3}\delta E_{40} \\ & + (J_{41})_{3,1}\delta\rho_{41} + (J_{41})_{3,2}\delta m_{41} + (J_{41})_{3,3}\delta E_{41}, \end{aligned} \tag{15}$$

where

$$\delta E_{41} = \frac{\delta P_{41}}{0.4} - \frac{0.5m_{41}^2}{\rho_{41}^2}\delta\rho_{41} + \frac{m_{41}}{\rho_{41}}\delta m_{41}. \tag{16}$$

The last row in the $(J_{41})_{row,col}$ submatrix, with designated subscripts, must be modified to create a new $(J_{41})_{row,col}$ submatrix, namely

$$
\begin{aligned}
(\tilde{J}_{41})_{3,1} &= (J_{41})_{3,1} - (J_{41})_{3,3}\left(\frac{0.5m_{41}^2}{\rho_{41}^2}\right) \\
(\tilde{J}_{41})_{3,2} &= (J_{41})_{3,2} + (J_{41})_{3,3}\left(\frac{m_{41}}{\rho_{41}}\right) \\
(\tilde{J}_{41})_{3,3} &= 0.
\end{aligned}
\tag{17}
$$

Under further simplification, the equations in (17) become

$$
\begin{aligned}
(\tilde{J}_{41})_{3,1} &= (J_{41})_{3,1} + \left(\frac{0.5m_{41}^3}{H\rho_{41}^3}\right) \\
(\tilde{J}_{41})_{3,2} &= (J_{41})_{3,2} - \left(\frac{m_{41}^2}{H\rho_{41}^2}\right) \\
(\tilde{J}_{41})_{3,3} &= 0.
\end{aligned}
\tag{18}
$$

These modifications must be made in the last row of the A matrix for proper implementation of the boundary conditions.

Since δP_{41} is the input point, the δP_{41} term of the δE_{41} equation in (11) may be absorbed into the B matrix, viz.

$$
B^T = \left[0 \; 0 \; . \; . \; . \; 0 \; \frac{-2.5m_{41}}{H\rho_{41}}\right]. \tag{19}
$$

The nonzero term in (19) is simply the coefficient on δP given in (16) and multiplied by $(J_{41})_{3,3}$. The state space model for the system is now completely defined. In the next section, the state space model is balanced, using the Schur method of balancing, and truncated. The resulting ROMs are then studied using the step and frequency responses.

Model Reduction

Obtaining an accurate reduced order model is very important for controller design, particularly for reducing the complexity of the resulting controller. No reliable techniques are currently available for reducing the order of the original nonlinear system while preserving large perturbation information. However, many methods are available for reducing the order of linear systems. Among these methods, the Schur method is a robust and well conditioned method to reduce the large state space models of gasdynamic systems. A reduced order model may be found directly by using projections defined by the left and right eigenspaces of the large eigenvalues of the product of the observability and controllability Grammians. Since the full order models are typically numerically ill-conditioned, some type of scaling is performed prior to model order reduction. A first consideration in choosing the ROM order is to view the largest HSVs of the system.

An abbreviated table of the 13 largest HSVs of the linear model of the NASA Lewis 40-60 inlet is shown in Figure 1.

order	HSV	ratio
1	1.0603e+01	
2	4.6175e+00	2.2962
3	1.9535e+00	2.3637
4	1.0341e+00	1.8891
5	4.9687e-01	2.0812
6	2.6303e-01	1.8890
7	9.2066e-02	2.8570
8	9.1363e-02	1.0077
9	2.1703e-02	4.2097
10	1.1679e-02	1.2926
11	1.6844e-03	6.9336
12	1.5313e-03	1.1000
13	1.5189e-04	10.0816

Figure 1. - Largest Hankel Singular Values of the NASA Lewis 40-60 Linear Inlet Model.

The ratio column in Figure 1 is simply the ratio of the HSV to the left of the number divided by the HSV above that number. A ROM is typically found by truncating the LFOM where there is a 10 to 1 break in the HSVs. At first glance the best break appears to be for a 12th order model. Other possible considerations include 8th and 10th order ROMs. It turns out that all of these ROMs trace the step response so close that they are not discernable on the graph. Subsequently, two other ROMs were calculated of order 4 and 6. Since the output is known to have a delay in its time response, the order of the model cannot be reduced much more than this. Even the 4th order model exhibits some oscillatory behavior when trying to represent the time delay. The step response for these two ROMs is shown in Figure 2. Also included in figure 2 are the step responses for the LFOM and the NLFOM. The 6th order model traces the actual LFOM response very close. As mentioned previously, the 4th order response is somewhat oscillatory during the time delay but still gives a reasonable approximation to the actual step response. For completeness, the frequency response is shown in Figure 3.

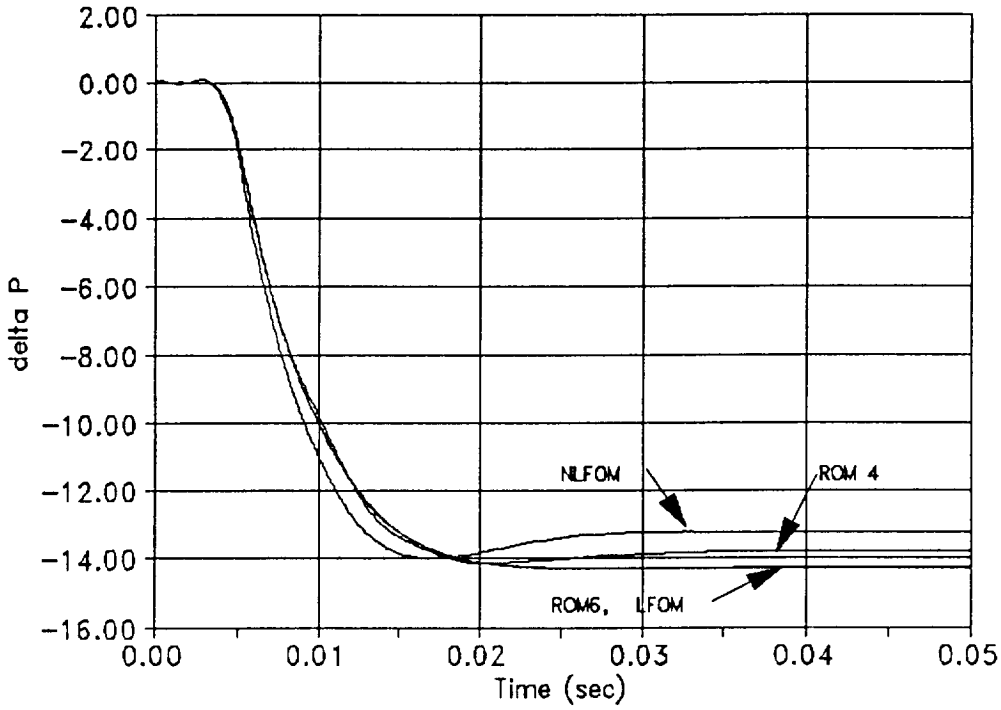

Figure 2 - Step Response of LFOM, NLFOM, and ROMs

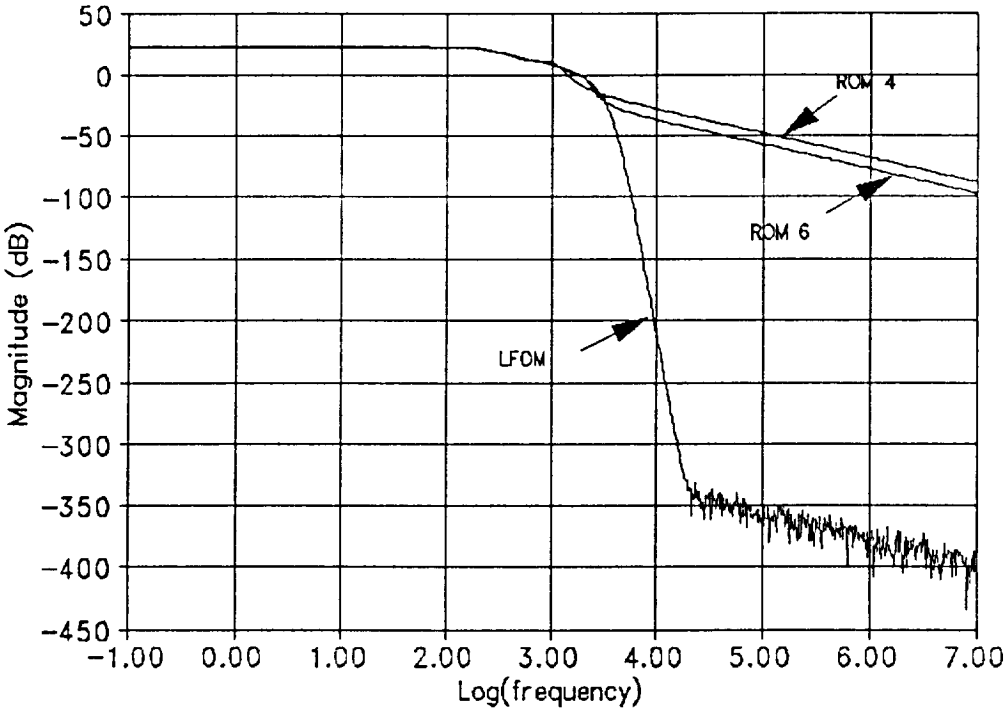

Figure 3 - Frequency Response for LFOM and ROMs

From Figure 3, it can be seen that the original linear system is very low pass. Notice that the frequency responses separate only when the system starts to attenuate. If higher order ROMs are considered, the only effect on the frequency response is that more roll-off is preserved by keeping more poles. Overall, the accuracy of the ROMs appear to be acceptable considering the amount of order reduction attempted. ROM4 is shown in Figure 4 while ROM6 is shown in Figure 5.

$$\left[\begin{array}{c|c} A & B \\ \hline C & D \end{array}\right] = \left[\begin{array}{cccc|c} -40.41 & 192.08 & -75.47 & 82.82 & -29.27 \\ -192.08 & -167.01 & 477.25 & -188.12 & -39.27 \\ -75.47 & -477.25 & -268.24 & 953.20 & -32.37 \\ -82.82 & -188.13 & -953.20 & -354.37 & -27.07 \\ \hline 29.27 & -39.27 & 32.37 & -27.07 & 0.00 \end{array}\right]$$

$$H(s) = \frac{3.70e{+}2s^3 - 1.18e{+}6s^2 + 1.74e{+}9s - 1.03e{+}12}{s^4 + 8.30e{+}2s^3 + 1.37e{+}6s^2 + 4.81e{+}8s + 7.51e{+}10}$$

Figure 4. - 4th order reduced order model for the NASA Lewis 40-60 Inlet

$$\left[\begin{array}{cccccc|c} -40.41 & 192.09 & -75.48 & 82.82 & -60.48 & 47.79 & -29.27 \\ -192.09 & -167.02 & 477.26 & -188.13 & 218.56 & -135.84 & -39.27 \\ -75.48 & -477.26 & -268.25 & 953.20 & -302.97 & 323.28 & -32.37 \\ -82.82 & -188.13 & -953.20 & -354.37 & 1155.66 & -352.32 & -27.07 \\ -60.48 & -218.56 & -302.97 & -1155.66 & -529.20 & 1655.41 & -22.93 \\ -47.79 & -135.84 & -323.28 & -352.32 & -1655.41 & -541.70 & -16.88 \\ \hline 29.27 & -39.27 & 32.37 & -27.07 & 22.93 & -16.88 & 0.00 \end{array}\right]$$

$$H(s) = \frac{1.29e{+}2s^5 - 9.44e{+}5s^4 + 3.59e{+}9s^3 - 8.12e{+}12s^2 + 1.06e{+}16s - 6.36e{+}18}{s^6 + 1.90e{+}3s^5 + 6.54e{+}6s^4 + 7.22e{+}9s^3 + 7.77e{+}12s^2 + 3.12e{+}15s + 4.45e{+}17}$$

Figure 5. - 6th order reduced order model for the NASA Lewis 40-60 Inlet

Conclusions

The given physical lumping method of differencing proved to be feasible for representing the dynamics of the NASA Lewis 40-60 inlet. An advantage of this differencing approach is that it readily allows the study of nonlinear model reduction methods, as the states are immediately available. This is not true of most other CFD methods. Furthermore, physical lumping is more intuitive. It is essentially a straight forward differencing approach which requires less up-front calculation than the split flux method presented in [1]. The resulting ROMs not only turned out to be of smaller order but they also efficiently captured the dynamics of the system. The Schur method of balancing proved to be a good choice for a model reduction scheme resulting in a substantial reduction in order from 123 to order 6 or smaller. Depending on the intended use of the reduced order models, the 6th order model appears practical for most purposes. The 4th order model may be used if time delay information is not important.

Acknowledgement

This research was partially supported by the Advanced Control Technology Branch of NASA Lewis Research Center via Grant NAG 3-904.

References

[1] Chicatelli, Amy, Methods for Developing Linear Reduced Order Models of Internal Flow Propulsion Systems, M. S. Thesis, The University of Akron, May 1990.

[2] Chicatelli, Amy, Hartley, Tom T., Methods for Developing Linear Reduced Models for Internal Flow Propulsion Systems, submitted to AIAA Journal of Propulsion and Power, Sept. 1990.

[3] Hartley, Tom T., A Simple Method for Simulating Gasdynamic Systems, Department of Electrical Engineering, The University of Akron, December 1990.

[4] Courant, Isaacson, and Rees, On the Solution of Nonlinear Hyperbolic Differential Equations by Finite Differences, Communications on Pure and Applied Mathematics, vol. V, 1952, pp. 243-255.

[5] Safonov, M. G., and Chiang, R. Y., A Schur Method for Balanced Truncation Model Reduction, IEEE Transactions on Automatic Control, vol. 34, No. 7, July 1989, pp. 729-733.

[6] Hurrell, H. G., Analysis of Shock Motion in Ducts During Disturbances in Downstream Pressure, NACA TN 4090, Sept. 1957.

[7] Roache, P. J., Computational Fluid Dynamics, Hermosa, Albuquerque, 1976.

[8] Varner, M. O., et al., Large Perturbation Flow Field Analysis and Simulation for Supersonic Inlets, NASA CR 174676, 1985.